Complete Prediction of the ^{1}H NMR Spectrum of Organic Molecules by DFT Calculations of Chemical Shifts and Spin–Spin Coupling Constants

Alessandro Bagno*[a]

Abstract: ^{1}H NMR chemical shifts and coupling constants for several aromatic and aliphatic organic molecules have been calculated with DFT methods. In some test cases (furan, *o*-dichlorobenzene and *n*-butyl chloride) the performance of several functionals and basis sets has been analyzed, and the various contributions to spin–spin coupling (Fermi-contact, diamagnetic and paramagnetic spin-orbit) have been evaluated. The latter two components cancel each other, so that the calculation of the contact term only is sufficient for an accurate evaluation of proton–proton couplings. Such calculated values are used to simulate the ^{1}H NMR spectra of organic molecules with complicated spin systems (e.g. naphthalene, *o*-bromochlorobenzene), obtaining a generally very good agreement with experimental spectra with no prior knowledge of the involved parameters.

Keywords: ab initio calculations · chemical shifts · NMR spectroscopy · spin–spin coupling

Introduction

Nuclear magnetic resonance (NMR) is probably the most powerful technique for structure determination in solution, since it can provide a wealth of data that can be related to chemical structure, conformation, and their relationship or interaction with the surroundings. The most fundamental data furnished by an NMR spectrum are chemical shifts (δ) and spin–spin coupling constants (J), and it is obviously desirable to relate these to chemical information. For common nuclei such as ^{1}H and ^{13}C there are many empirical correlations between δ or J and chemical structure and conformation covered in basic NMR textbooks.[1] As such, their scope may not span molecular species with an unusual electronic structure, such as strained molecules or reactive intermediates, or even stable molecules outside the scope of such relationships; for less common heteronuclei such knowledge is much more limited.

Even when dealing with stable, well-behaved species, however, there may still be a long way to go before an NMR spectrum can be completely assigned. This applies especially to ^{1}H NMR spectra, which often contain several (and frequently overlapping) strongly coupled spin systems (small $\Delta\nu/J$ ratio) giving rise to a complex multiplet pattern, as is often the case for aromatic systems and long aliphatic chains. This difficulty can only be partly alleviated by running the spectrum at a higher field, since many spin systems contain chemically equivalent but magnetically non-equivalent spins which will yield a second-order spectrum under all conditions. Whereas one could simulate the spin system,[1] and hence extract chemical shifts and coupling constants, in practice the NMR characterization of new molecules often contains just a chemical shift range, together with the familiar "multiplet" statement, to denote any part of the spectrum that cannot be visually interpreted under first-order rules. Likewise, even though the familiar array of multidimensional techniques is extremely helpful in elucidating through-bond connectivities, all such techniques require some independent assignments to be made first.

Obviously, if all chemical shifts and couplings were independently available, one could just simulate all the spin systems in the molecule, no matter their complexity, and obtain a calculated NMR spectrum which can be compared to the experimental one. In this paper, we present a computational protocol aimed at this prediction.

The calculation of the chemical shift requires a calculation of the isotropic nuclear shielding tensor $\boldsymbol{\sigma}$; efficient implementations of such algorithms within ab initio and density-functional (DFT) methods, are now available. The reader is referred to a recent comprehensive review for details of the theory and applications.[2] Such theoretical tools are widely applied nowadays. In particular, it is known that the shielding of light nuclei (notably ^{1}H and ^{13}C) can be accurately calculated.[3] DFT methods have been especially successful in this respect, and it has recently been shown that such calculations can attain "chemical accuracy".[4]

[a] Dr. A. Bagno
Centro CNR Meccanismi Reazioni Organiche
Dipartimento di Chimica Organica, Università di Padova
via Marzolo 1, 35131 Padova (Italy)
Fax: (+39)0498275239
E-mail: alex@chor.unipd.it

0947-6539/01/0708-1652 $ 17.50+.50/0

In contrast, the calculation of spin–spin coupling constants is comparatively less advanced, and much of the recent literature has been concerned with theoretical and methodological issues.[2, 5] Lately, however, the calculations of J has been used as a tool for investigating structural or conformational problems;[6–19] this field of research has recently received further strong impetus from the discovery that J-coupling can be transmitted through hydrogen bonds.[20–28] A finite (albeit very small) spin–spin coupling is predicted also for dispersion-bound complexes.[29] Other recent developments are the calculation of the solvent effect on NMR parameters by continuum methods,[30–32] relativistic calculations for heavy elements,[33, 34] and the investigation of the tensor properties of J by NMR in liquid crystals.[35, 36]

According to Ramsey's formulation, spin–spin coupling arises from several electron–nuclear interactions, that is the Fermi-contact (FC), paramagnetic spin-orbit (PSO), diamagnetic spin-orbit (DSO) and spin-dipole (SD) terms. Details of the theory and calculation of these terms have been extensively reviewed.[2, 5] We only recall a few points, that is a) for light nuclei, the FC term is often the most important one; b) the PSO and DSO terms (which may be larger or smaller than the FC term) often tend to cancel each other; c) the SD term is generally negligible. These remarks suggest that the calculation of the FC term might be enough for a correct estimation of $^1H-^1H$ coupling constants. This approach has in fact been successfully employed[15, 18, 25, 27] in the calculation of couplings involving ^{13}C, ^{15}N and ^{11}B.

The FC interaction is very sensitive to electron correlation and structural effects, and Hartree–Fock theory is inherently of little value for this calculation.[2, 5] Hence, various correlated methods for the calculation of spin–spin couplings have been developed and applied, which can be broadly categorized as multiconfiguration SCF (CASSCF),[6–9, 22, 31, 34–36] coupled-cluster (EOM-CCSD),[10–13] configuration interaction (QCISD),[17, 18] Møller-Plesset[19] and density-functional (DFT)[14–16, 24–27, 29, 30, 33, 37] theory.

Some issues related to the basis sets for such calculations need to be mentioned.[2, 38] The FC interaction is transmitted by electrons in s-type orbitals, which have a large density at the nucleus. If core orbitals are involved, these may not be well described by typical energy-optimized basis sets (which rather emphasize the valence region). Furthermore, the functional form of Gaussian basis functions (with a maximum rather than a cusp) at the nucleus is not correct. Use of basis sets augmented with "tight" s functions (having exponents of 10^4-10^5), especially in connection with CASSCF theory, has been advocated to remedy these basis-set deficiencies.[2, 38] However, DFT results have provided good calculated J values at a moderate computational cost for several light nuclei, both in covalent[14–16] and hydrogen-bonded[24–27, 37e–f] species using conventional basis sets. Also, Ziegler recently pointed out that the FC interaction is essentially a valence property, with core orbitals playing a minor role.[39] Perera and Bartlett[11] calibrated basis sets for best performance with regard to the quality of the wave function at the nuclei, and emphasized the need for a flexible representation of outer-core, inner-shell valence region. Therefore, even though the problem of basis set quality is still open to further investigation, all approaches can achieve a good level of accuracy. DFT methods with conventional high-quality Gaussian basis sets seem to provide an accurate and convenient framework for such investigations and, owing to their very favorable scaling properties with molecular size, they hold great promise for the investigation of biomolecules, which still pose formidable problems to the experimental NMR spectroscopist, and for which the use of other correlated methods would be too expensive.[16]

With these ideas in mind, we have strived to provide a computational protocol generally applicable for the calculation of proton chemical shifts and couplings in organic molecules, in order to simulate the NMR spectrum from such calculated δ and J values and compare it with the experimental values. A similar approach was earlier adopted for vinyllithium[6] and fluoroethylene.[7] We emphasize at this point that spectrum simulation is employed to provide a calculated NMR spectrum starting from computed shifts and couplings, rather than (as is usually intended) to obtain the same data from an experimental spectrum.

As a first step, we have focussed on rigid aromatic molecules, thus avoiding conformational effects while maintaining complex spin systems. An example of aliphatic compounds and related problems will also be given.

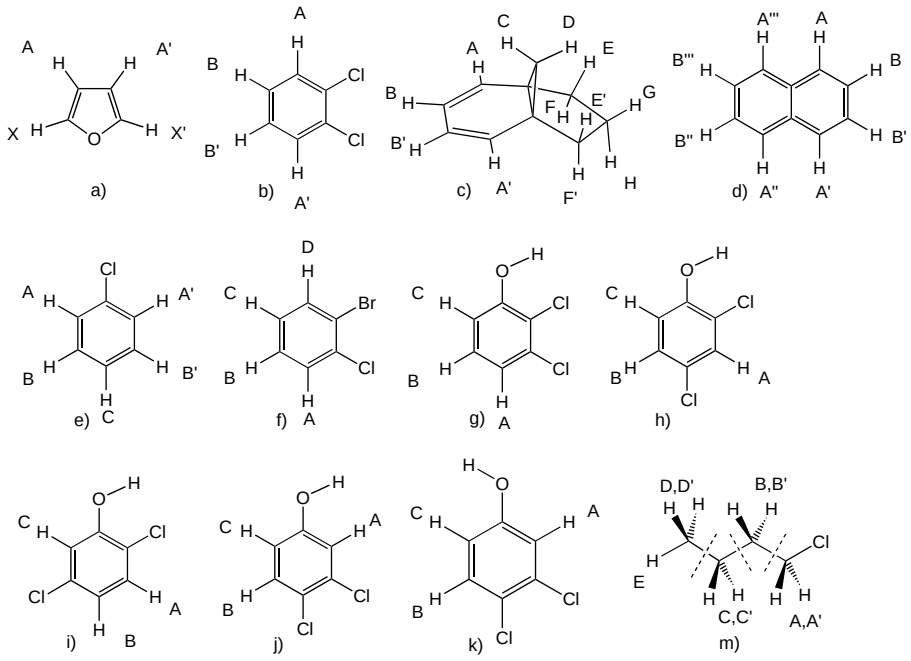

Scheme 1. Different spin systems discussed in this paper.

Results

Since our goal is to establish a generally applicable computational protocol, which should be hopefully extended to a wide array of organic species, attention must be paid in reaching an acceptable compromise between accuracy and practical feasibility. It should also be kept in mind that experimental spectra are often solvent-dependent, and that the accuracy of spectral simulation will depend on the quality of the experimental data. For these reasons, experimental spectra presented herein were purposely obtained with a routine instrument (200 MHz), and $CDCl_3$ was used as solvent. Finally, since under ordinary resolution conditions an accuracy of about 0.1 ppm for shifts and 0.2 Hz for couplings can be expected, we did not seek agreement between experimental and calculated values to better than this threshold.

In this work, we have only dealt with ^{1}H NMR chemical shifts and couplings. Nuclear shieldings have been calculated with the GIAO method,[2, 3] and converted to chemical shifts as $\delta = \sigma_{ref} - \sigma$.

The calculation of coupling constants should in principle include all its major contributions, that is FC, PSO and DSO, in order to evaluate their relative magnitude. To this effect, we firstly tested two organic molecules (furan and *o*-dichlorobenzene) using *deMon-NMR*,[37] which can calculate all the above contributions within density functional theory. These calculations (including IGLO nuclear shieldings for consistency) were run with the Perdew–Wang exchange with Perdew correlation functional[40] (P86) and the IGLO-III basis set[37] at the B3LYP/6-31G(d,p) geometry. An integration grid with 64 points of quadrature was used. The FC contribution is calculated by finite perturbation theory (FPT) [Eq. (1)]:

$$J_{MN} = \left(\frac{\mu_0}{4\pi}\right)^2 \frac{\hbar}{2\pi} \left(\frac{8\pi\beta}{3}\right)^2 \frac{1}{a_0^6} \gamma_M \gamma_N \frac{1}{\lambda} B_{FC} \qquad (1)$$

where B_{FC} is the Fermi-contact term in au, λ is the applied perturbation (see below), γ_M and γ_N the magnetogyric ratios the involved nuclei, and the other symbols have the usual meaning.[37e] Thus, placing the perturbation on nucleus M allows to detect spin–spin coupling to all remaining nuclei in the molecule, for example nucleus N. In principle, the calculated coupling constant is insensitive to the actual value of λ (which was recommended to be 10^{-3} au)[37e] and to placing the perturbation on either nucleus (i.e., $J_{MN} = J_{NM}$), but care was taken to ensure consistency in the results (see below).

Since it became apparent that the PSO and DSO contributions cancel each other to within 0.1 Hz (see below), we then proceeded for the remaining cases with the sole calculation of the FC contribution (by FPT) with *Gaussian 98*.[41] The following functionals were used: the popular Becke's hybrid three-parameter functional with Lee–Yang–Parr correlation (B3LYP)[42] and the one-parameter functional with modified Perdew–Wang exchange and Perdew–Wang 1991 correlation as modified by Barone and Adamo (MPWPW91).[43] The basis sets used were 6-31G or 6-311G (especially for geometry optimization) or Dunning's correlation-consistent cc-pVTZ, variously augmented. Several combinations of method, basis set, and optimization level were tested, and are denoted by boldface numbers in the Table for TMS (Table 1). Tight SCF convergence criteria were always employed. It was always verified that the calculated coupling constants did not appreciably depend on the choice of the perturbed centre, with differences below 0.1 Hz. When B_{FC} is small (weak coupling, as is often the case for the molecules dealt with herein) the numerical accuracy becomes too low using the recommended value; therefore, in most calculations we used a value of 10^{-2} au, after verifying in several instances that large J values were within ± 0.2 Hz using both $\lambda = 10^{-2}$ and 10^{-3} au.

Table 1. Combinations of method, basis set, and optimization level used in the calculations, and nuclear shieldings of TMS (ppm).

Index	Level	σ[a]
1[b]	P86/IGLO-III//B3LYP/6-31G(d,p)	31.29
2	HF/6-311G(d,p)//HF/6-311G(d,p)	32.47
3	HF/6-311G(2d,2p)//HF/6-311G(d,p)	32.20
4	B3LYP/6-31G(d,p)//B3LYP/6-31G(d,p)	31.76
5	B3LYP/6-311G(d,p)//B3LYP/6-311G(d,p)	32.00
6	B3LYP/6-311++G(2d,2p)//B3LYP/6-311G(d,p)	31.72
7	B3LYP/D95++(2d,2p)//B3LYP/6-311G(d,p)	31.67
8	B3LYP/cc-pVTZ//B3LYP/6-311G(d,p)	31.66
9	B3LYP/aug-cc-pVTZ//B3LYP/6-311G(d,p)	31.65
10	B3LYP/cc-pVTZ//B3LYP/6-31G(d,p)	31.62
11	MPWPW91/6-311++G(2d,2p)//B3LYP/6-31G(d,p)	31.53
12	MPWPW91/cc-pVTZ//B3LYP/6-31G(d,p)	31.46

[a] Average of individual shieldings (ppm). [b] Run with *deMon*-NMR. All remaining calculations run with *Gaussian 98*.

Since we are concerned with ^{1}H–^{1}H couplings ($\gamma_H = 2.675220 \times 10^8\ s^{-1}T^{-1}$), all the constants in Equation (1) are defined and J_{HH} (Hz) $= 75740.19 B_{FC}$, if $\lambda = 10^{-2}$ au. The overall protocol then amounts to: a) geometry optimization; b) shielding calculation; c) a series of FC calculations in which the perturbation is placed on all but one magnetically non-equivalent protons.

NMR spectra were eventually simulated using calculated or experimental chemical shifts and coupling constants with the *Mestre-C* program.[44] In most cases, a line width of 0.5 Hz was assumed, and all calculated couplings smaller than 0.2 Hz were set to zero in the simulation.

As a first step, we ran a series of calculations for the reference standard TMS and two model spin systems (AA′XX′), that is furan and *o*-dichlorobenzene (ODCB). The former is used as a textbook example, giving rise to a "deceptively simple" pair of distorted triplets which may be mistaken for an A_2X_2 spectrum, and the latter is often used for calibrating the spectrometer resolution.

Effect of tight *s* functions: This was firstly tested for in the case of the geminal coupling ($^2J_{HH}$) in methane[45] (Table 2). At the B3LYP/cc-pVTZ level (with B3LYP/6-31G(d,p) geometry; level **10**), addition of a single *s* function with exponent 10^5 to hydrogen atoms (level **10a**) leads to a small (0.4 Hz) improvement in the calculated coupling constant. In the case of furan (Table 3b), minor changes (± 0.2 Hz) were again observed for $J_{AA'}$ and J_{AX}. Hence, even though the effect may be noticeable, and often goes in the right direction, its magnitude seems too

0947-6539/01/0708-1654 $ 17.50+.50/0 *Chem. Eur. J.* **2001**, *7*, No. 8

Table 2. Basis set effect, including the use of tight *s* functions, on the geminal coupling ($^2J_{HH}$) in methane.

Level	σ (H)	δ (H)	$^2J_{HH}$
6	31.49	0.23	– 12.3
10	31.42	0.20	– 11.0
10a[a]	–	–	– 11.4
exptl		0.23[b]	– 12.564[c]

[a] cc-pVTZ augmented with a single *s* function ($\alpha = 10^5$) on hydrogen atoms. The energy is not affected by this added basis function.[38] [b] Ref. [46]. [c] Ref. [47].

small to justify an extended use of this approach, especially in larger molecules, and this was not further pursued.

Furan: Experimental[48] and calculated (at levels **1**–**10**) chemical shifts and coupling constants (Hz) are summarized in Tables 3 and 4 (see Scheme 1). Let us firstly concentrate on the individual contributions to spin–spin couplings in Table 4. For all four coupling constants, the magnitude of the PSO and DSO contributions is comparable to, or even larger than the FC one.[16] However, they almost exactly cancel each other, the net result being that the total *J* value is essentially that of the FC contribution.

Table 3 also show that HF calculations (**2**–**3**) fare rather well with regard to calculated shieldings, whereas all coupling constants are grossly overestimated. On the contrary, all DFT calculations (**1**, **4**–**12**) lead to coupling constants lying essentially in the correct range and resulting in good $\Delta\nu/J$ values, even though they differ in the individual shift values. A series of spectra simulated with chemical shifts and couplings calculated at several computational levels (**6**, **8**, **11**) or the experimental values is plotted in Figure 1. All calculated spectra have the correct "triplet-like" appearance.

Table 3. Method and basis set effect on calculated chemical shifts[a] (top) and spin–spin couplings[b] (bottom) of furan (Scheme 1a).

Level	σ (A,A′)	σ (X,X′)	δ (A,A′)	δ (X,X′)	Δδ	Δν AX[c]
1	24.72	23.53	6.57	7.76	1.19	357
2	26.04	25.04	6.43	7.43	1.00	300
3	25.67	24.68	6.53	7.52	0.99	297
4	25.35	24.28	6.41	7.48	1.07	321
5	25.53	24.51	6.47	7.49	1.02	306
6	25.12	24.07	6.60	7.65	1.05	315
7	24.87	23.83	6.80	7.84	1.04	312
8	25.10	24.11	6.55	7.55	1.00	300
9	25.03	24.00	6.62	7.65	1.03	309
10	25.05	24.05	6.57	7.57	1.00	300
11	24.96	23.92	6.57	7.61	1.04	312
12	24.93	23.94	6.53	7.52	0.99	297
exptl	–	–	6.37	7.42	1.05	315

Level	$^3J_{AA'}$	$^3J_{AX}$	$^4J_{A'X}$	$^4J_{XX'}$	$\Delta\nu/J_{AX}$	$\Delta\nu/J_{A'X}$
1[d]	3.1	1.4	0.8	1.2	255	297
2[e]	37.1	50.0	– 42.4	54.5	6.0	7.1
3[e]	39.4	53.8	– 45.4	59.0	5.5	6.5
4[f]	3.0; 3.3	2.3; 2.4	0.8; 0.6	1.5; 1.6	140	535
5[g]	2.9	1.9	0.6	1.2	161	510
6	3.1	2.0	0.7	1.4	157	450
7	1.0	0.15	0.6	1.4	2080	520
8	2.8	1.7	0.7	1.4	176	428
9	2.8	1.8	0.6	1.3	172	515
10	2.8	1.7	0.7	1.4	176	428
10a	3.0	1.5	–	–	200	–
11	3.0	1.6	0.8	1.1	195	390
12	2.6	1.3	0.8	1.1	228	371
exptl	3.5	1.8	0.8	1.5	175	394

[a] In ppm. [b] Experimental data from ref. [48]. [c] In Hz, at 300 MHz. [d] Sum of FC, PSO, DSO contributions. [e] $\lambda = 10^{-3}$ au. [f] First and second entry calculated with $\lambda = 10^{-3}$ and 10^{-2} au, respectively. [g] All calculations from this level on run with $\lambda = 10^{-2}$ au.

Table 4. Components of spin–spin couplings of furan at level **1**.

	FC	PSO	DSO	Total
$^3J_{AA'}$	3.2	1.0	– 1.1	3.1
$^3J_{AX}$	1.6	1.1	– 1.3	1.4
$^4J_{A'X}$	0.9	2.2	– 2.3	0.8
$^4J_{XX'}$	1.2	2.4	– 2.4	1.2

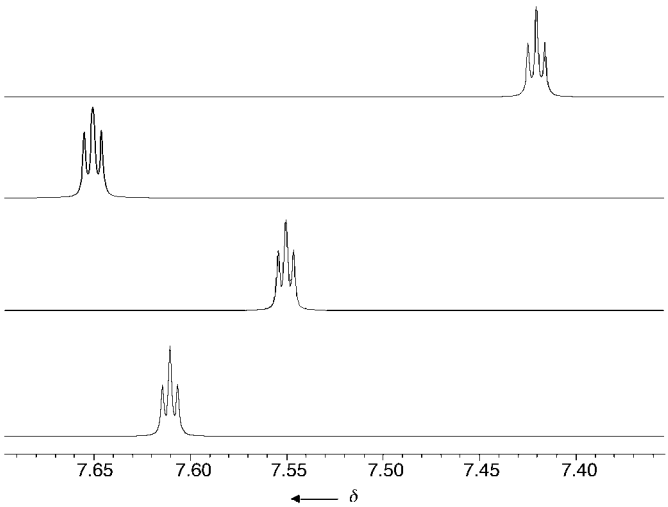

Figure 1. Simulated XX′ subspectrum of furan (300 MHz, line width 0.5 Hz). Top to bottom: using experimental chemical shifts and couplings, or using calculated data: B3LYP/6-311++G(2d,2p)//B3LYP/6-311G(2d,2p) level (**6**); B3LYP/cc-pVTZ//B3LYP/6-311G(2d,2p) (**8**); MPWPW91/cc-pVTZ//6-31G(d,p) (**11**).

***o*-Dichlorobenzene**: The same series of calculations seen before was run also in this case (see Scheme 1b and Tables 5 and 6). The same conclusions also apply for furan, taking into account the fact that this system is in general more demanding, owing to the smaller couplings involved. Calculated and experimental[48] spectra are compared in Figure 2 for the levels **10** and **12**.

At this point it is worthwhile to make a preliminary assessment. a) Calculated shieldings are not overly sensitive to method and basis set, except in low-level HF calculations (**2**–**3**). b) Geometry optimization with the inexpensive 6-31G(d,p) basis is adequate for reproducing all trends. c) The most demanding calculation is that of the coupling constants. In this respect, we note the almost exact (to within 0.2 Hz) cancellation of the PSO and DSO terms, which justifies the sole calculation of the FC term from this point on. d) For a meaningful calculation a DFT method is necessary (the poor results of Hartree–Fock theory are again borne out) and, in general, the cc-pVTZ basis set seems superior to 6-311++G(2d,2p).[38] Augmenting the basis with diffuse functions has a negligible effect.

Table 5. Method and basis set effect on calculated chemical shifts[a] and spin–spin couplings[b] of *o*-dichlorobenzene (Scheme 1b).[a]

Level	σ (A,A′)	σ (B,B′)	δ (A,A′)	δ (B,B′)	Δδ	Δν AB
1	23.59	23.99	7.70	7.30	0.40	120
2	24.88	25.06	7.59	7.41	0.18	54
3	24.33	24.64	7.87	7.56	0.30	90
4	24.41	24.59	7.35	7.17	0.18	54
5	24.59	24.82	7.41	7.18	0.23	69
6	24.00	24.36	7.72	7.36	0.36	108
7	24.03	24.34	7.64	7.33	0.31	93
8	24.07	24.37	7.59	7.29	0.30	90
9	23.98	24.29	7.66	7.36	0.30	90
10	24.02	24.32	7.60	7.30	0.30	90
11	23.82	24.20	7.64	7.26	0.38	114
12	23.88	24.20	7.58	7.26	0.32	96
exptl	–	–	7.37	7.11	0.26	78

Level	$^3J_{AB}$	$^5J_{AA'}$	$^4J_{AB'}$	$^3J_{BB'}$	$\Delta\nu/J_{AB}$	$\Delta\nu/J_{AB'}$
1[b]	7.3	0.0	1.6	6.5	16	75
2	−0.8	−9.8	10.6	−1.5	67	5.1
3	−1.5	−9.8	12.1	−2.3	60	7.4
4	7.6	0.8	1.5	6.8	7.1	36
5	7.2	0.3	1.1	6.6	15	98
6	7.8	0.3	1.1	7.0	14	98
7	5.0	0.4	1.3	4.3	19	71
8	7.3	0.2	1.2	6.5	12	75
9	7.0	0.2	1.3	6.3	13	69
10	7.2	0.3	1.3	6.4	12	69
11	7.3	0.2	1.4	6.5	16	81
12	6.7	0.1	1.4	5.9	14	69
exptl	8.1	0.3	1.5	7.5	9.7	52

[a] See footnotes [a] and [b] to Table 3. Calculations at levels **2**–**4** and **5**–**12** run with $\lambda = 10^{-3}$ and $\lambda = 10^{-2}$ au, respectively. [b] Sum of FC, PSO, and DSO contributions.

Table 6. Components of spin–spin couplings of *o*-dichlorobenzene at level **1**.

	FC	PSO	DSO	Total
$^3J_{AB}$	7.5	0.1	−0.3	7.3
$^5J_{AA'}$	0.05	1.7	−1.8	0.02
$^4J_{AB'}$	1.6	1.8	−1.8	1.6
$^3J_{BB'}$	6.7	0.2	−0.4	6.5

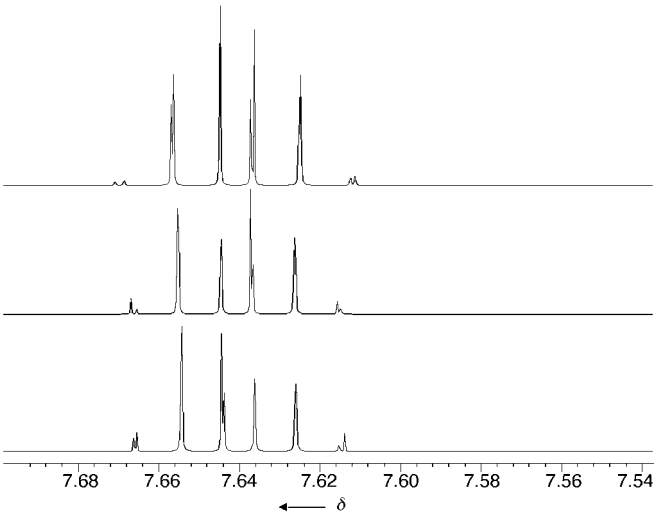

Figure 2. Simulated BB′ subspectrum of *o*-dichlorobenzene (300 MHz, line width 0.05 Hz). Top to bottom: using experimental chemical shifts and couplings, or using calculated data: B3LYP/cc-pVTZ//B3LYP/6-31G(d,p) (**10**); MPWPW91/cc-pVTZ//6-31G(d,p) (**12**). In this case only, the spectra have been displaced for clarity, so that equivalent peaks are aligned.

Based on these considerations, the study was further extended to a series of spin systems exhibiting spectral patterns which are difficult to disentangle visually. All the following calculations were performed at level **10** (B3LYP/cc-pVTZ at B3LYP/6-31G(d,p) geometry).

1,3-Diolefin system: Günther[49] investigated in depth the AA′BB′ spin system of bicyclic, conformationally rigid 1,3-cyclohexadienes; we selected the carbocyclic example depicted in Scheme 1c. Spectral simulation[49] led to the experimental values reported in Table 7 (for the olefinic region only), together with the corresponding values calculated herein. The

Table 7. Chemical shifts and coupling constants of Günther's diolefin, naphthalene, chlorobenzene and *o*-bromochlorobenzene (Schemes 1c–f).[a]

Günther's diolefin[b]		Naphthalene		Chlorobenzene		*o*-Bromochlorobenzene[c]	
δ (A)	6.38 (6.07)	δ (A)	8.09 (7.86)	δ (A,A′)	7.54	δ (A)	7.60 (7.45)
δ (B)	6.08 (5.71)	δ (B)	7.71 (7.50)	δ (B,B′)	7.48	δ (B)	7.32 (7.24)
$^3J_{AB}$	8.6 (9.25)	$^3J_{AB}$	7.4	δ (C)	7.39	δ (C)	7.27 (7.11)
$^3J_{BB'}$	5.2 (5.94)	$^3J_{BB'}$	6.0	$^4J_{AA'}$	1.97	δ (D)	7.69 (7.61)
$^4J_{AB'}$	0.2 (0.58)	$^4J_{AB'}$	0.9	$^3J_{AB}$	7.19	$^3J_{AB}$	7.1 (8.0)
$^5J_{AA'}$	1.5 (1.31)	$^4J_{AA'''}$	−0.4	$^5J_{AB'}$	0.38	$^4J_{AC}$	1.2 (1.5)
		$^5J_{AA'}$	0.7	$^4J_{AC}$	0.91	$^5J_{AD}$	0.2 (0.0)
		$^5J_{AA''}$	0.8	$^4J_{BB'}$	1.36	$^3J_{BC}$	6.4 (ca. 8.0)
		$^5J_{AB''}$	0.2	$^3J_{BC}$	6.51	$^4J_{BD}$	1.2 (1.8)
		$^5J_{A'''B}$	0.2			$^3J_{CD}$	7.2 (7.7)
		$^6J_{AB'''}$	−0.2				
		$^6J_{A''B}$	−0.1				
		$^6J_{BB''}$	0.1				
		$^7J_{BB'''}$	0.2				

[a] Calculated data at level **10**; $\lambda = 10^{-2}$ au. Chemical shifts and coupling constants in ppm and Hz, respectively. All couplings smaller than 0.2 Hz have been set to zero in the simulations. If applicable, experimental data are given in parentheses after the calculated value. [b] Experimental data from ref. [49]. Only the olefinic part is reported. [c] Experimental shifts and coupling constants assuming first-order analysis (see Discussion).

spectra simulated with the experimental and calculated parameters are compared in Figure 3. For the sake of completeness, the calculations were extended to the aliphatic region of the spectrum (originally not reported), where the two noteworthy features are: a) a sizable coupling constant (1.0 Hz) is predicted for $^4J_{CF}$ in the W-shaped arrangement, as expected, whereas the corresponding $^4J_{DF}$ is much smaller (−0.4 Hz); b) the calculated shift of H_C is negative ($\delta = -0.60$), as expected for a proton lying in the shielding region above a π system.

Naphthalene and other aromatics: Naphthalene (see Scheme 1d) provides a very complicated AA′A″A‴BB′B″B‴ system, and also offers the opportunity to calculate more long-range couplings in the W-shaped arrangement (e.g. $^5J_{AA''}$).

0947-6539/01/0708-1656 $ 17.50+.50/0 *Chem. Eur. J.* **2001**, *7*, No. 8

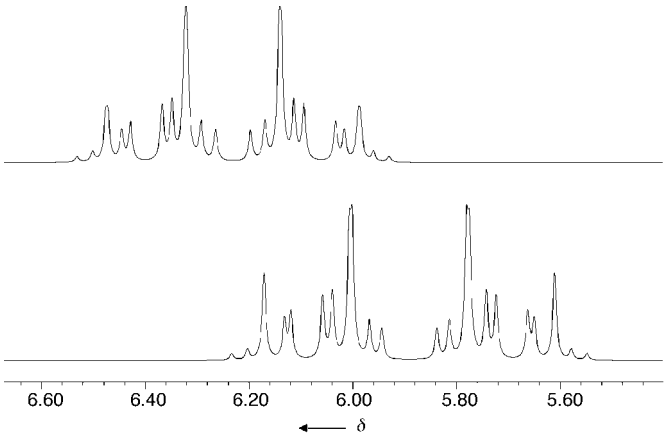

Figure 3. Calculated (top) and experimental (bottom) spectrum of Günther's 1,3-diolefin (see Scheme 1c); olefinic AA′BB′ part only (60 MHz, line width 0.5 Hz, level **10**).

Calculated data are collected in Table 7; the experimental and simulated spectra are compared in Figure 4.

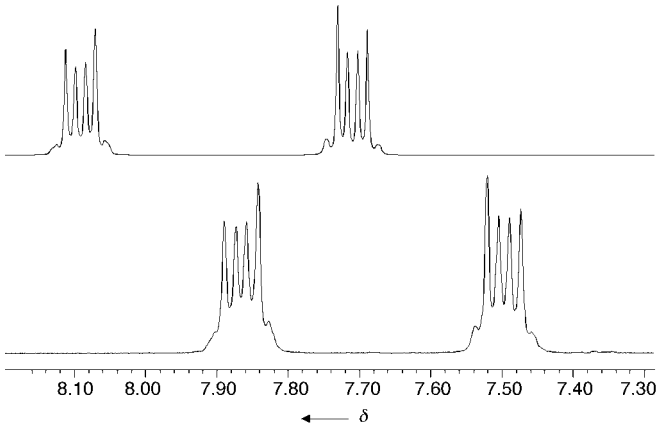

Figure 4. Calculated (top) and experimental (bottom) spectrum of naphthalene (200 MHz, line width 0.5 Hz, level **10**).

Chlorobenzene and *o*-bromochlorobenzene (Scheme 1e–f) give rise to strongly coupled AA′BB′C or ABCD systems, respectively; see Table 7 and Figure 5 and Figure 6.

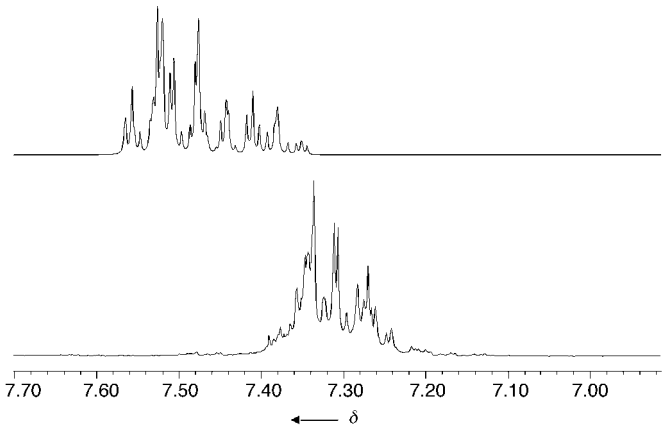

Figure 5. Calculated (top) and experimental (bottom) spectrum of chlorobenzene (see caption to Figure 4).

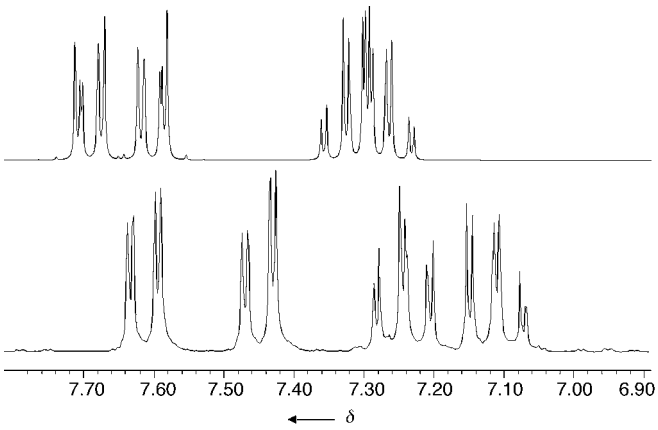

Figure 6. Calculated (top) and experimental (bottom) spectrum of *o*-bromochlorobenzene (see caption to Figure 4).

The different substitution patterns available for dichlorophenols (DCP) may give rise to AMX (2,3-, 2,4-, 2,5- and 3,4-DCP) or A_2B (2,6- and 3,5-DCP) systems. This offers an opportunity to distinguish the different isomers on the basis of the calculated spectrum. The calculations have been run for the four isomers giving AMX systems. Preliminary semi-empirical (AM1) calculations showed that the most stable conformers of 2,3-, 2,4- and 2,5-DCP (Scheme 1g–i) have the OH group pointing towards the chlorine atom in the 2-position, and this geometry was used as starting point for further optimization. In the case of 3,4-DCP there is no such arrangement, so that two conformations, differing by the O–H bond orientation, have been considered (Scheme 1j–k). A possible solvent effect on the experimental spectrum was tested for by running the spectra also in acetone as solvent, where however the spectra were essentially unchanged. The data are collected in Table 8 and compared in Figure 7, Figure 8, Figure 9 and Figure 10.

An examination of the experimental spectrum of 3,4-DCP (lowest trace in Figure 10) and the calculated one for conformer 1 (Scheme 1j) shows a reversal in the ordering of the most shielded signals, although the magnitude of coupling constants is essentially correct. This is simply an effect due to the conformation of the O–H bond, since in conformer 2 (Scheme 1k) the ordering is correct, albeit exaggerated, and

Table 8. Chemical shifts and coupling constants of dichlorophenols (DCP; Scheme 1g–k).[a]

2,3-DCP		2,4-DCP		2,5-DCP		3,4-DCP[b]	
δ (A)	7.11	δ (A)	7.42 (7.46)	δ (A)	7.32 (7.23)	δ (A)	6.94 (6.96)
δ (B)	7.23	δ (B)	7.28 (7.29)	δ (B)	6.95 (6.86)	δ (B)	7.40 (7.29)
δ (C)	7.04	δ (C)	7.08 (7.08)	δ (C)	7.16 (7.04)	δ (C)	6.62 (6.69)
$^3J_{AB}$	7.2	$^4J_{AB}$	2.2 (2.2)	$^3J_{AB}$	7.8 (8.8)	$^5J_{AB}$	0.3 (0.0)
$^3J_{AC}$	1.2	$^5J_{AC}$	0.2 (0.0)	$^5J_{AC}$	0.2 (0.0)	$^4J_{AC}$	2.6 (2.9)
$^4J_{BC}$	7.3	$^3J_{BC}$	7.9 (8.8)	$^4J_{BC}$	2.2 (2.2)	$^3J_{BC}$	7.6 (8.8)

[a] See footnote [a] to Table 7. [b] Calculated data are the average for the two conformers (Scheme 1j, k; see text).

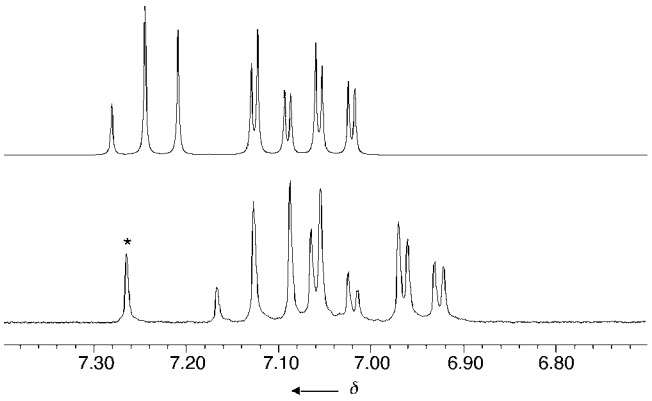

Figure 7. Calculated (top) and experimental (bottom) spectra of 2,3-dichlorophenol (see caption to Figure 4). The asterisk denotes solvent.

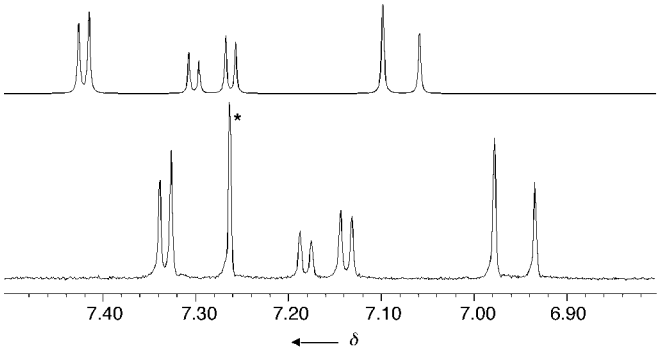

Figure 8. Calculated (top) and experimental (bottom) spectra of 2,4-dichlorophenol (see caption to Figure 4). The asterisk denotes solvent.

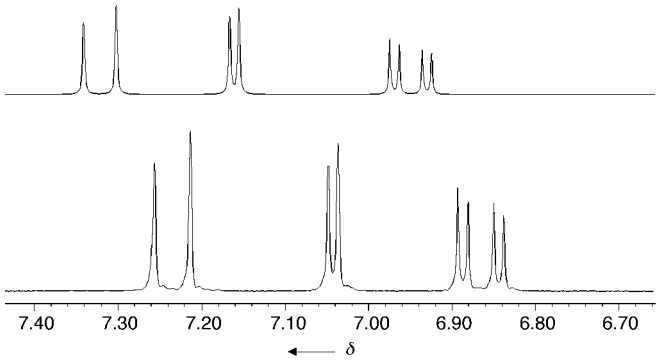

Figure 9. Calculated (top) and experimental (bottom) spectra of 2,5-dichlorophenol (see caption to Figure 4).

the coupling constants are not affected. Since these two conformers are equal in energy (<0.1 kcal mol^{-1} at the B3LYP/cc-pVTZ level), it is meaningful to average their data (see Table 8), which leads to an excellent agreement with the experimental spectrum.

***n*-Butyl chloride as a test case for aliphatic systems**: Aliphatic systems present the obvious difficulty that several conformers may have to be investigated in order to arrive at a reliable prediction. We restricted the investigation to a linear aliphatic *n*-butyl chain. If the conformation is assumed to be blocked in an *anti* arrangement, the spin system can be represented as AA′BB′CC′DD′E (Scheme 1m). Since this molecule differs substantially in geometry, bonding etc. from the aromatics

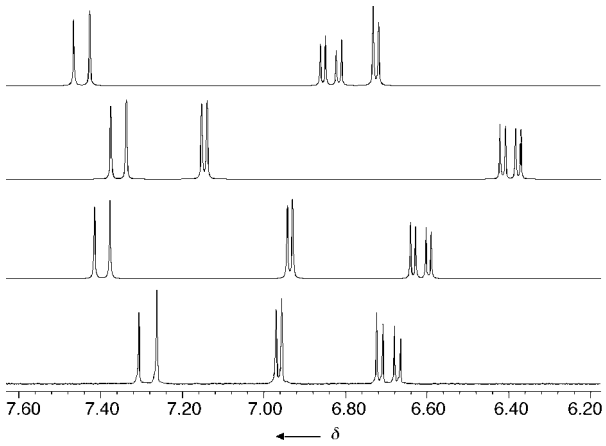

Figure 10. Calculated and experimental spectra of 3,4-dichlorophenol (see caption to Figure 4). Top to bottom: calculated spectra for conformation 1, 2, average (see text), and experimental.

dealt with so far, we repeated the complete calculation of all contributions to spin–spin coupling as observed before (Tables 9 and 10). It is apparent that the PSO and DSO contributions again cancel out to an extent similar to that previously seen for aryl derivatives.

Table 9. Chemical shifts and coupling constants of *n*-butyl chloride (Scheme 1m).[a]

	Level 1	Level 10	Level 10 (av.)[b]
δ (A,A′)	3.54	3.49	3.49 (3.54)
δ (B,B′)	1.73	1.72	1.72 (1.76)
δ (C,C′)	1.30	1.25	1.25 (1.47)
δ (D,D′)	0.91	0.93	1.02[c] (0.94)
δ (E)	1.20	1.21	–
$^2J_{AA'}$	−8.0	-8.8	–
$^3J_{AB}$	4.3	4.3	8.1 (6.6)
$^3J_{AB'}$	12.6	12.0	–
$^2J_{BB'}$	−10.4	-11.3	–
$^3J_{BC}$	3.5	3.5	7.8 (ca. 8)
$^3J_{BC'}$	12.6	12.0	–
$^2J_{CC'}$	−10.6	−11.4	–
$^3J_{CD}$	3.6	3.7	8.6[c] (7.3)
$^3J_{CD'}$	14.0	13.5	–
$^3J_{CE}$	3.0	3.3	–
$^3J_{DD'}$	−10.5	−10.8	–
$^2J_{DE}$	−10.8	−11.5	–

[a] See footnote [a] to Table 7. All calculated ^4J and ^5J are <0.2 Hz. [b] Averages used in the simulation (see text). [c] Average of D, D′ and E.

Table 10. Components of largest spin–spin couplings of *n*-butyl chloride at level **1**.

	FC	PSO	DSO	Total
$^2J_{AA'}$	−8.23	2.19	−2.00	−8.04
$^3J_{AB}$	4.32	0.23	−0.21	4.34
$^3J_{AB'}$	12.63	2.63	−2.67	12.59
$^2J_{BB'}$	−10.64	1.96	−1.74	−10.41
$^3J_{BC}$	3.49	0.31	-0.33	3.46
$^3J_{BC'}$	12.61	2.68	−2.69	12.60
$^2J_{CC'}$	−10.74	2.14	−1.98	−10.58
$^3J_{CD}$	3.63	0.51	-0.56	3.57
$^3J_{CD'}$	13.99	2.80	−2.82	13.97
$^3J_{CE}$	3.07	0.44	−0.50	3.01
$^3J_{DD'}$	−10.66	2.73	−2.56	−10.50
$^2J_{DE}$	−11.01	2.82	−2.66	−10.84

0947-6539/01/0708-1658 $ 17.50+.50/0 *Chem. Eur. J.* **2001**, *7*, No. 8

As expected, the spectrum calculated under these assumptions (not shown) does not have the correct appearance. On the other hand, a full conformational averaging will lead to an $A_2B_2C_2D_3$ system and consequently to the loss of AA′, BB′ etc. couplings. Hence, for this simulation chemical shifts and coupling constants for each chemically distinct site (A, B, C, D) were averaged; the results of the simulation are in Figure 11, which indeed has the familiar appearance.

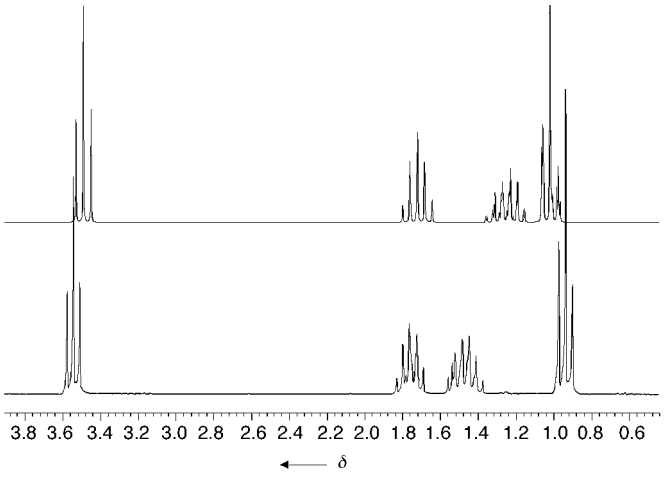

Figure 11. Calculated (top) and experimental (bottom) spectrum of *n*-butyl chloride (see caption to Figure 4). All shifts and coupling constants for each chemically non-equivalent site were averaged.

Discussion

The results obtained in this work can be evaluated as follows. Calculated chemical shifts and couplings should, first of all, lie in the appropriate region for every type of functional group and substitution pattern. Secondly, the chemical shift difference ($\Delta\nu$) between chemically non-equivalent protons should be considered, since this parameter will determine the overall look of the spectrum. Finally, the $\Delta\nu/J$ ratio at a given field will cause the spin system to be first- or second-order and hence determine the fine detail (number of lines and their intensities) in the spectrum. In the cases where such data were available, we compared our calculated results with those obtained by spectral fitting of experimental data, although this is not necessary, since the availability of shifts and couplings makes it possible to obtain a completely calculated NMR spectrum which can be visually compared with the experimental one.

A variety of theoretical methods has been tested on TMS, furan and ODCB. It is then apparent that the calculation of proton chemical shifts poses few if any problems, in that calculated δ values (even at the HF level) lie within 0.5 ppm of the experimental value.[3] This may even be considered an "exact" agreement if one recalls that solvent effects of this magnitude are common. The situation is obviously improved if one only considers shifts relative to a component of the spin system, (i.e., displacing the whole spectrum). In this case, as one would expect, the agreement is better (<0.1 ppm), as illustrated in Figures 1 and 2.

With regard to calculated spin–spin coupling constants, the general conclusion that can be drawn from our results is that proton–proton couplings are, in practice, dominated by the Fermi-contact term, so that the calculation of this term alone suffices for predicting a *J* value lying within a few tenths of Hz of the experimental value. It is, however, very important to stress that the PSO and DSO terms are, by themselves, generally not negligible at all, and may even be larger than the FC term. It is rather their *cancellation* that lies at the root of the good agreement between the FC term and experimental values. This cancellation has been found to hold for proton couplings in both aromatic and aliphatic molecules, but it must of course be carefully tested to cover the desired scope, for example when investigating couplings with other nuclei.

DFT calculations perform remarkably well without augmenting the basis set with tight *s* functions. In fact, while in the case of methane ($^2J_{HH}$) such augmentation (levels **10** vs **10a**) does lead to a small improvement (ca. 4%), in the case of furan the effect, despite being larger (ca. 10%), has opposite signs for $J_{AA'}$ and J_{AX}. Therefore, judging also from the good results obtained in the remaining cases (see below), it seems that within the scope of the present method tight *s* functions do not necessarily lead to improved calculated values.

The capability to predict the NMR spectrum correctly is measured by the $\Delta\nu/J$ ratio, which of course includes inaccuracies in both shielding and coupling calculations. An examination of Tables 3 and 5 allows to conclude that level **10** (B3LYP/cc-pVTZ//B3LYP/6-31G(d,p)) yields the least deviation between all calculated and experimental couplings, which forms the basis for our use of this particular combination in all further cases. In any event, the IGLO-III, 6-311++G(2d,2p) and cc-pVTZ basis sets, in connection with the P86, B3LYP or MPWPW91 functionals (levels **1**, **6**, **10**, **11**, **12**) perform rather similarly, so the choice among them is not definitive.

We finally note that the level used for geometry optimization does not seem to have a large influence on the final outcome, provided it is at least as good as B3LYP/6-31G(d,p), which is affordable for small- and medium-sized molecules.

The results obtained for several complicated aromatic systems, that is Günther's 1,3-diolefin, naphthalene, chlorobenzene, and *o*-bromochlorobenzene (Figure 3-6), are indicative of the predictive power of the computational protocol we have described. Thus, the AA′BB′ pattern experimentally found for Günther's 1,3-diolefin is well reproduced computationally, and a visual comparison allows one to note the good agreement with respect to the number, location and intensity of the lines. The only small discrepancy arises because the calculated $\Delta\nu_{AB}$ value (18 rather than 22 Hz at 60 MHz) is somewhat too small, which is reflected in a smaller separation of the AA′ and BB′ subspectra.

One can also note that the calculated spectrum is too deshielded. This feature is found in all spectra calculated in this work, and is probably related to a solvent effect acting consistently in this direction, so that the general features are not affected.

Likewise, the 8-line naphthalene pattern is readily borne out from the calculated spectrum, with an excellent agreement in the $\Delta\nu_{AB}$ value (calcd: 76 vs 72 Hz at 200 MHz), without any prior knowledge or analysis of the NMR data.

Known trends in the relative magnitude of couplings are also reproduced, such as the sizable long-range coupling $^5J_{AA''}$ (0.8 Hz) because of the W-shaped arrangement of the nuclei.[1]

The spectrum of chlorobenzene (an AA′BB′C system) is very complicated, and certainly difficult to analyze by inspection. Nevertheless, the calculated spectrum reproduces the general features of this irregular multiplet (Figure 5).

o-Bromochlorobenzene provides an ABCD spin system. The most deshielded A and D protons are clearly separated from B and C, but their separation is too large, whereas the predicted separation between B and C is too small, and therefore with a larger distortion in the relative intensities. However, the general appearance of the spectrum is, again, clearly recognizable. Peak assignment ($\delta(D) > \delta(A) > \delta(B) > \delta(C)$) is also possible without recourse to assumptions or empirical data. A simple first-order analysis of the experimental spectrum (i.e., assuming $J_{AD} = 0$ and $J_{AB} \approx J_{BC}$) leads to the coupling constants in Table 7. The agreement is fairly good, although some caution with regard to the experimental values is in order owing to the approximate analysis.

Grant et al.[48] analyzed this spectrum as an AA′BB′ system, which is only approximately valid. (At 60 MHz the AD and BC frequency differences are small, that is 5 and 3 Hz, respectively, with respect to $\Delta\nu_{AB} = 12.3$ Hz, which justifies this assumption). This analysis led to the values of J_o (AB, CD $\equiv$ AB, and BC $\equiv$ BB′) = 8.6, J_m (AC, BD $\equiv$ AB′) = 2.5, and J_p (AD $\equiv$ AA′) = 0.3 Hz. These are somewhat different from our calculated values; however, given the good agreement found with our own experimental results seen above, we are inclined to believe that the disagreement is largely due to the low resolution of the original spectrum, and consequently of the fit quality.

As readily seen from the spectra of Figures 7–10, 2,3-DCP gives rise to an ABC system, whereas 2,4-, 2,5- and 3,4-DCP give rise to AMX systems with $J_{AX} = 0$. The general features of the 2,3-DCP ABC spectrum are, again, essentially reproduced computationally, although the chemical shift difference between H_B (H-5) and H_A, H_C (H-4, H-6) is somewhat too large. With regard to the three AMX systems, one can easily note the good agreement with experimental spectra, with the correct ordering of peaks and closely similar couplings. We recall that for 3,4-DCP, where the dominance of a single conformation of the O–H group cannot be assumed, the agreement is reached only averaging the two conceivable conformations (see Results). In general, we also note that an appreciable, albeit small, *para* coupling is calculated (ca. 0.2 Hz), which is not experimentally found. However, since under ordinary resolution conditions such small couplings easily go undetected, very accurate experiments are needed to ascertain whether the calculated value is actually overestimated.

For flexible molecules such as aliphatic chains, the spin system cannot be described in terms of a rigid, fixed conformation. Thus, in general, a full conformational analysis should be performed on the system. Even so, CH_2 protons remain magnetically non-equivalent, since a X-CH_2-CH_2-Y system is strictly AA′XX′ and such spectra may look like AA′XX′ or A_2X_2 depending on the actual chemical shifts and couplings. Since it is beyond the scope of this work to fully explore conformational effects on the spectra of flexible chains, we only wish to emphasize the following points. a) Even the simple assumption of chemical shifts and couplings being averaged among chemically equivalent sites leads to a correct representation of the experimental spectrum of *n*-butyl chloride. b) The cancellation between the PSO and DSO terms appears to hold also for aliphatic systems, although of course more data would be needed for an assessment. The averaging over shifts and couplings should not affect this cancellation, since Fukui et al. showed that all major contributions to $^3J_{HH}$ in ethane have the same conformational dependence.[19] Thus, the computational treatment of such flexible systems may be more complicated, but probably will not by itself introduce new difficulties.

Conclusion

The DFT calculation of ^{1}H nuclear shieldings and spin–spin coupling constants in organic molecules can be efficiently performed. The results presented herein show that the calculation of the Fermi-contact term is generally sufficient for a dependable estimation of ^{1}H couplings, although this is due to a cancellation of the other two major terms (paramagnetic and diamagnetic spin-orbit), and the scope of this cancellation effect has, perhaps, to be investigated in more depth. We have also found that, among the various combinations of DFT methods and basis sets, NMR calculations (shieldings and couplings) run at the B3LYP/cc-pVTZ level and B3LYP/6-31G(d,p) geometry seem to yield a good compromise between accuracy and cost. At the computer power currently available, such calculations are feasible within quite reasonable time limits (e.g., ca. 42 hours for *o*-bromochlorobenzene with a 750 MHz Pentium III under Linux for the whole protocol), whereby an extension to larger systems looks straightforward.

The data calculated this way can be directly employed to simulate the ^{1}H NMR spectrum at a given frequency, and such simulated spectra generally compare very favorably with the experimental spectra. Hence, such calculations can complement the usual array of NMR techniques for structure elucidation, since they provide a new standpoint for establishing the relationship between NMR parameters and chemical structure or conformation. In a more practical way, they can help the synthetic chemist in sorting out the possible products of a new reaction by comparing an experimental spectrum with the spectra predicted for a few viable alternatives.

Acknowledgement

Part of this work was carried out on an SGI Origin 2000, with computer time granted by CINECA. The author thanks V. G. Malkin and O. L. Malkina for providing the *deMon-NMR* and for helpful suggestions.

[1] H. Günther, *NMR Spectroscopy*, 2nd ed., Wiley, Chichester, **1992**.
[2] T. Helgaker, M. Jaszuński, K. Ruud, *Chem. Rev.* **1999**, *99*, 293.

  0947-6539/01/0708-1660 $ 17.50+.50/0

[3] a) D. B. Chesnut, *Annu. Rep. NMR Spectrosc.* **1994**, *29*, p. 71; b) A. C. de Dios, *Progr. Nucl. Magn. Spectrosc.* **1996**, *29*, 229; c) D. B. Chesnut in *Reviews in Computational Chemistry*, *Vol. 8* (Eds.: K. B. Lipkowitz, D. B. Boyd), VCH, New York, **1996**; d) J. F. Stanton, J. Gauss, H.-U. Siehl, *Chem. Phys. Lett.* **1996**, *262*, 183; e) H. Fukui, *Progr. Nucl. Magn. Spectrosc.* **1997**, *31*, 317.
[4] a) C. Adamo, V. Barone, *Chem. Phys. Lett.* **1998**, *298*, 113; b) M. Bienati, C. Adamo, V. Barone, *Chem. Phys. Lett.* **1999**, *311*, 69.
[5] H. Fukui, *Prog. Nucl. Magn. Reson. Spectrosc.* **1999**, *35*, 267.
[6] K. Ruud, T. Helgaker, P. Jorgensen, K. L. Bak, *Chem. Phys. Lett.* **1994**, *226*, 1.
[7] T. Helgaker, M. Jaszuński, K. Ruud, *Mol. Phys.* **1997**, *91*, 881.
[8] M. Pecul, J. Sadlej, *Chem. Phys.* **1999**, *248*, 27.
[9] M. Pecul, M. Jaszuński, J. Sadlej, *Chem. Phys. Lett.* **1999**, *305*, 139.
[10] a) S. A. Perera, R. J. Bartlett, P. von R. Schleyer, *J. Am. Chem. Soc.* **1995**, *117*, 8476; b) S. A. Perera, R. J. Bartlett, *J. Am. Chem. Soc.* **1996**, *118*, 7849; c) S. A. Perera, R. J. Bartlett, *J. Am. Chem. Soc.* **2000**, *122*, 1231; d) J. E. Del Bene, S. A. Perera, R. J. Bartlett, *J. Am. Chem. Soc.* **2000**, *122*, 3560.
[11] S. A. Perera, M. Nooijen, R. J. Bartlett, *J. Chem. Phys.* **1996**, *104*, 3290.
[12] V. Galasso, *Int. J. Quantum Chem.* **1998**, *70*, 313.
[13] R. D. Wigglesworth, W. T. Raynes, S. Kirpekar, J. Oddershede, S. P. A. Sauer, *J. Chem. Phys.* **2000**, *112*, 3735.
[14] G. Cuevas, E. Juaristi, A. Vela, *J. Phys. Chem. A* **1999**, *103*, 932.
[15] T. Onak, J. Jaballas, M. Barfield, *J. Am. Chem. Soc.* **1999**, *121*, 2850.
[16] J. Czernek, J. Lang, V. Sklenár, *J. Phys. Chem. A* **2000**, *104*, 2788.
[17] I. Carmichael, *J. Phys. Chem.* **1993**, *97*, 1789.
[18] a) I. Carmichael, D. M. Chipman, C. A. Podlasek, A. S. Serianni, *J. Am. Chem. Soc.* **1993**, *115*, 10863; b) F. Cloran, I. Carmichael, A. S. Serianni, *J. Phys. Chem. A* **1999**, *103*, 3783; c) F. Cloran, I. Carmichael, A. S. Serianni, *J. Am. Chem. Soc.* **2000**, *122*, 396; d) F. Cloran, Y. Zhu, J. Osborn, I. Carmichael, A. S. Serianni, *J. Am. Chem. Soc.* **2000**, *122*, 6435.
[19] H. Fukui, H. Inomata, T. Baba, K. Miura, H. Matsuda, *J. Chem. Phys.* **1995**, *103*, 6597.
[20] A concise summary, and references up to 1999, of this exciting new field can be found in: G. Gemmecker, *Angew. Chem.* **2000**, *112*, 1276; *Angew. Chem. Int. Ed.* **2000**, *39*, 1224.
[21] A. Liu, A. Majumdar, W. Hu, A. Kettani, E. Skripkin, D. J. Patel, *J. Am. Chem. Soc.* **2000**, *122*, 3206.
[22] M. Pecul, J. Sadlej, *Chem. Phys. Lett.* **1999**, *308*, 486.
[23] M. Pecul, J. Leszczynski, J. Sadlej, *J. Chem. Phys.* **2000**, *112*, 7930.
[24] C. Scheurer, R. Brüschweiler, *J. Am. Chem. Soc.* **1999**, *121*, 8661.
[25] A. J. Dingley, J. E. Masse, R. D. Peterson, M. Barfield, J. Feigon, S. Grzesiek, *J. Am. Chem. Soc.* **1999**, *121*, 6019.
[26] a) N. S. Golubev, I. G. Shenderovich, S. N. Smirnov, G. S. Denisov, H.-H. Limbach, *Chem. Eur. J.* **1999**, *5*, 492; b) H. Benedict, I. G. Shenderovich, O. L. Malkina, V. G. Malkin, G. S. Denisov, N. S. Golubev, H.-H. Limbach, *J. Am. Chem. Soc.* **2000**, *122*, 1979.
[27] A. Bagno, *Chem. Eur. J.* **2000**, *6*, 2925.
[28] J. E. Del Bene, M. J. T. Jordan, *J. Am. Chem. Soc.* **2000**, *122*, 4794.
[29] F. R. Salsbury, R. A. Harris, *Mol. Phys.* **1998**, *94*, 307.
[30] V. G. Malkin, O. L. Malkina, G. Steinbrunner, H. Huber, *Chem. Eur. J.* **1996**, *2*, 452.
[31] K. V. Mikkelsen, K. Ruud, T. Helgaker, *J. Comput. Chem.* **1999**, *20*, 1281.
[32] M. Pecul, J. Sadlej, *Chem. Phys.* **2000**, *255*, 137.
[33] J. Khandogin, T. Ziegler, *J. Phys. Chem. A* **2000**, *104*, 113.
[34] L. Visscher, T. Enevoldsen, T. Saue, H. J. Aa. Jensen, J. Oddershede, *J. Chem. Phys.* **2000**, *112*, 3493.
[35] P. Lantto, J. Kaaski, J. Vaara, J. Jokisaari, *Chem. Eur. J.* **2000**, *6*, 1395, and previous papers by the same group.
[36] D. L. Bryce, R. E. Wasylishen, *J. Am. Chem. Soc.* **2000**, *122*, 3197.
[37] a) D. R. Salahub, R. Fournier, P. Mlynarski, I. Papai, A. St-Amant, J. Ushio in *Density Functional Methods in Chemistry* (Eds.: J. Labanowski, J. Andzelm), Springer, New York, **1991**; b) A. St-Amant, D. R. Salahub, *Chem. Phys. Lett.* **1990**, *169*, 387; c) V. G. Malkin, O. L. Malkina, M. E. Casida, D. R. Salahub, *J. Am. Chem. Soc.* **1994**, *116*, 5898; d) V. G. Malkin, O. L. Malkina, L. A. Eriksson, D. R. Salahub, *Modern Density Functional Theory: A Tool For Chemistry*, *Vol. 2* (Eds.: J. M. Seminario, P. Politzer), Elsevier, Amsterdam, **1995**; e) V. G. Malkin, O. L. Malkina, D. R. Salahub, *Chem. Phys. Lett.* **1994**, *221*, 91; f) O. L. Malkina, D. R. Salahub, V. G. Malkin, *J. Chem. Phys.* **1996**, *105*, 8793.
[38] T. Helgaker, M. Jaszuński, K. Ruud, A. Górska, *Theor. Chem. Acc.* **1998**, *99*, 175.
[39] J. Khandogin, T. Ziegler, *Spectrochim. Acta* **1999**, *55A*, 607.
[40] a) J. P. Perdew, Y. Wang, *Phys. Rev. B* **1986**, *33*, 8800; b) J. P. Perdew, *Phys. Rev. B* **1986**, *33*, 8822.
[41] *Gaussian 98*, *Revision A.7*, Gaussian, Inc., Pittsburgh PA, **1998**.
[42] A. D. Becke, *J. Chem. Phys.* **1993**, *98*, 5648.
[43] C. Adamo, V. Barone, *J. Chem. Phys.* **1998**, *108*, 664.
[44] C. Cobas, J. Cruces, F. J. Sardina, *MestRe-C 2.2*, *Magnetic Resonance Companion NMR Data Processing Program*, Universidad de Santiago de Compostela, Spain, **2000**, http://qobrue.usc.es/jsgroup/MestRe-C/MestRe-C.html.
[45] J. Geertsen, J. Oddershede, W. T. Raynes, G. E. Scuseria, *J. Magn. Reson.* **1991**, *93*, 458.
[46] H. Friebolin, *Basic One- and Two-Dimensional NMR Spectroscopy*, VCH, Weinheim, **1993**.
[47] F. A. L. Anet, D. J. O'Leary, *Tetrahedron Lett.* **1989**, *30*, 2755.
[48] D. M. Grant, R. C. Hirst, H. S. Gutowsky, *J. Chem. Phys.* **1963**, 38, 470.
[49] H. Günther, H. H. Hinrichs, *Ann. Chem.* **1967**, *706*, 1.

Received: October 6, 2000 [F2783]